The UBIRIS.v2: A Database of Visible Wavelength Iris Images Captured On-the-Move and At-a-Distance

Hugo Proença, Sílvio Filipe,
Ricardo Santos, João Oliveira, and
Luís A. Alexandre

Abstract—The iris is regarded as one of the most useful traits for biometric recognition and the dissemination of nationwide iris-based recognition systems is imminent. However, currently deployed systems rely on heavy imaging constraints to capture near infrared images with enough quality. Also, all of the publicly available iris image databases contain data correspondent to such imaging constraints and therefore are exclusively suitable to evaluate methods thought to operate on these type of environments. The main purpose of this paper is to announce the availability of the UBIRIS.v2 database, a multisession iris images database which singularly contains data captured in the visible wavelength, at-a-distance (between four and eight meters) and on on-the-move. This database is freely available for researchers concerned about visible wavelength iris recognition and will be useful in accessing the feasibility and specifying the constraints of this type of biometric recognition.

Index Terms—Iris recognition, biometrics, noncooperative image acquisition, visible-light iris images, covert recognition.

✦

1 INTRODUCTION

THE idea of using the iris texture to discriminate between individuals came from Bertillon and is over 100 years old. In 1987, Flom and Safir obtained the first patent for an automated iris recognition process, and few years later, Daugman published a method that is the basis of near all of the currently deployed systems. Due to favorable comparisons with other biometric traits, the popularity of the iris has grown considerably over recent years and substantial attention has been paid by both commercial and governmental organizations. Nationwide applications are starting to be deployed (e.g., border control in the United Kingdom[1] and United Arab Emirates[2]). These large applications are regarded as a grand challenge for the pattern recognition community. As an illustration, over 50 percent of the publications cited in a recent iris recognition survey [3] were published since 2005.

Currently, deployed systems rely on good quality images, captured in a stop-and-stare interface, at close distances and using near infrared (700-900 nm) wavelengths. As reported in a study conducted by *Aton Origin* for the United Kingdom Passport Service [1], these imaging constraints are a major obstacle for the massification of iris-based biometric systems. Here, when compared to other traits, the iris scored relatively low, due to the excessive time and effort demanded of subjects in the data acquisition process.

Further advances in iris recognition technologies are needed to meet the full range of operational requirements, which essentially

_____

1. http://www.ukba.homeoffice.gov.uk/managingborders/technology/iris/.

2. http://portal.acm.org/citation.cfm?id=1347658.

_____

● *The authors are with the Departamento de Informática, Universidade da Beira Interior, Rua Marquês DAvila e Bolama, 6201-001 Covilhã, Portugal. E-mail: {hugomcp, sfilipe, rsantos, joliveira, lfbaa}@di.ubi.pt.*

focus on the handling of nonideal biometric samples. In this context, the National Institute of Standards and Technology has recently promoted a challenge [23] that focused this problem and gave access to a set of nonideal near infrared (NIR) images. Simultaneously, several attempts to perform iris recognition in the visible wavelength were made, although it is considered that the resulting captured data impose limits to the recognition feasibility (e.g., stronger lighting sources should be needed to appropriately capture strong pigmented irises). However, the specification of these limits remains to be done.

In 2004, we released the UBIRIS [25] database. Our purpose was to *simulate* less constrained imaging processes and acquire visible wavelength images with several types of data occluding the iris rings (considered *noise*). A large number of experiments were conducted on this database and reported in the literature, although the realism of its noise factors received some criticisms. This was a major motivation for the development of a new version of the database (UBIRIS.v2) in which the images were *actually* captured in nonconstrained conditions (at-a-distance, on-the-move, and on the visible wavelength), with correspondingly more realistic noise factors.

The major purpose of the UBIRIS.v2 database is to constitute a new tool to evaluate the feasibility of visible wavelength iris recognition under far from ideal imaging conditions. In this scope, the various types of nonideal images, imaging distances, subject perspectives, and lighting conditions existent on this database could be of strong utility in the specification of the visible wavelength iris recognition feasibility and constraints.

The remainder of this paper is organized as follows: Section 2 briefly overviews the iris recognition technology and discusses the challenges that arise from less constrained environments. A detailed description of the announced database is given in Section 3. Section 4 reports our experiments and discusses the results. Section 5 informs about the database availability, and finally, Section 6 presents the conclusions.

2 IRIS RECOGNITION

With some minor exceptions, the large majority of the published iris recognition methods follow the statistical pattern recognition paradigm and can be divided into four separable stages: segmentation, normalization, feature extraction, and comparison (classification).

The process starts with the segmentation of the region correspondent to the iris ring in the close-up eye image. Further, to compensate for varying pupils' sizes, imaging distances, and distortions, the data are transformed into a double dimensionless polar coordinate system, through a process known as the *Daugman Rubber Sheet*. Regarding the feature extraction stage, existing approaches can be roughly divided into one of three variants: phase-based methods (e.g., [6]), zero-crossing methods (e.g., [2]), and texture-analysis methods (e.g., [30]). Daugman [6] used multiscale quadrature wavelets to extract texture phase information and obtain an iris signature with 2,048 binary components. Boles and Boashash [2] computed the zero-crossing representation of a 1D wavelet at different resolutions of concentric circles. Wildes [30] proposed the characterization of the iris texture through a Laplacian pyramid with four different levels (scales). Finally, in the feature comparison stage, a numeric dissimilarity value is produced which determines the subjects' identity. Here, it is usual to apply different distance metrics (Hamming [6], euclidean [13] or weighted euclidean [17]), or methods based on signal correlation [30].

The accuracy of the deployed iris recognition systems is remarkable. In a study of 200,000,000,000 cross comparisons conducted by Daugman [7], he reported false acceptance rates of order 10^{-6} with false rejections of 1 percent. Other independent evaluations ([15] and [18]) confirm this accuracy.

2.1 Less Constrained Image Acquisition

The human iris is an internal organ, naturally protected, visible from the exterior, and enables contactless data acquisition which, together with the face, propitiates the potential advantage of being covertly used. Assuming that covert iris-based recognition systems will inevitably constitute a trade-off between data acquisition constraints and recognition accuracy, the challenge is to maximally increase flexibility in three axes: subjects' position and movements, imaging distances, and lighting conditions. This area has received growing interest from the research community and constituted the scope of several recent publications. Among others, the "Iris-on-the-move" project [19] should be highlighted. The goal is to acquire images while subjects walk at normal speed through an access control point. *Honeywell Technologies* applied for a patent of a similar system,[3] able to perform at-a-distance iris recognition. Previously, Fancourt et al. [10] showed that it is possible to acquire images at-a-distance of up to 10 meters with sufficient quality to support iris recognition, and Narayanswamy et al. [21] increased the iris imaging depth-of-field through a simple framework composed by a camera with fixed focus, without a zoom lens. Park and Kim [24] proposed an approach to fast at-a-distance acquisition of in-focus iris images, and He et al. [12] and Boyce et al. [4] studied the acquisition of in-focus images and analyzed the role of the different wavelengths in the recognition error rates. Although concluding that illumination inside the 700-900 nm optimally reveals the richness of the iris structure, they observed that irises with moderate levels of pigmentation could be imaged in the visible light with good quality.

Recently, the analysis of the quality of the data captured in less constrained conditions became the focus of several research works. Chen et al. [5] quantified the local data quality based on a set of bidimensional wavelets. Kalka et al. measured several image quality factors that were later fused according the Dempster-Shafer theory. Schuckers et al. [28] proposed the use of projection techniques to compensate for distorted and occluded iris images resulting from off-angle image acquisition.

2.2 Iris Image Databases

There are currently seven free available iris image databases that can be used for biometric purposes: Chinese Academy of Sciences (CASIA [14], with three distinct versions), Multimedia University (MMU [20], two versions), University of Bath (BATH [29]), University of Olomuc (UPOL [9]), Iris Challenge Evaluation (ICE versions of 2005 and 2006 [22]), West Virginia University (WVU [27]), and University of Beira Interior (UBIRIS [25]), for which main characteristics are given in Table 1. At first, it should be stressed that, with the exceptions of the UPOL (imaged with an optometric device) and UBIRIS databases, all of the databases contain NIR images. Also, none of the data sets contain images acquired at largely varying distances and all of them used a rigid image acquisition protocol. Finally, excluding the UBIRIS database, the remaining databases contain very moderate levels and types of noisy data.

3 DESCRIPTION OF THE UBIRIS.v2 DATABASE

When planning the UBIRIS.v2 database, we had three basic concerns: to acquire images, first, of moving subjects, second, at varying imaging distances, and finally, to incorporate noise factors that realistically result from nonconstrained and varying lighting environments.

Anticipating that the levels of iris pigmentation should play an important role in the recognition feasibility, we classified the captured images into three categories, according to this criterium: "light," "medium," and "heavy" pigmented. As the average luminance in the iris regions varies inversely with the levels of

iris pigmentation, this criterium was used to make the partition of the complete set of images into each category. The "light" category contains the blue and light green irises and the highest luminance values (average μ_Y and standard deviation σ_Y values of, respectively, 51.95 and 3.90), "medium" contains the light and medium brown and the dark green irises ($\mu_Y = 37.70, \sigma_Y = 3.15$), and finally, "heavy" contains the dark brown and almost black irises ($\mu_Y = 29.46, \sigma_Y = 2.25$).

3.1 Imaging Framework and Setup

The setup of the imaging framework is given in Table 2. As illustrated in Fig. 1, this framework was installed in a lounge under both natural and artificial lighting sources. We placed several marks on the floor (between 3 and 10 meters away from the acquisition device) and asked for volunteers for the image acquisition processes. Two distinct image acquisition sessions were performed, one each during two weeks and separated by an interval of one week. From the first to the second session, the location and orientation of the acquisition device and artificial light sources were changed in order to increase heterogeneity. Volunteers were, in large majority, Latin Caucasian (around 90 percent) and also black (8 percent) and Asian people (2 percent). Around 60 percent of the volunteers performed both imaging sessions, while 40 percent performed exclusively one, either during the first or second acquisition period.

Subjects were required to walk at a slightly slower than normal speed and to look at several lateral marks that obliged them to rotate head and eyes, enabling the manual capturing of three images per meter, between 8 and 4 meters, giving a total of 15 images per eye and session for the large majority of the individuals. It should be stressed that this requested cooperative behavior had the unique purpose of normalizing the number of usable images per subject and imaging session. A completely covert procedure could have been used, with a necessarily lower number of usable images per session. As illustrated in Fig. 2, the significantly higher range of distances between the subjects and the imaging framework is one of the major distinguishable points between the UBIRIS.v2 database and the other databases.

3.2 Nonideal Images

The image acquisition process plays a major role in the quality of the captured data, which dictates the overall system's accuracy. Also, it is expectable that less intrusive image acquisition processes decrease the quality of the captured data and increase its heterogeneity. Through visual inspection, we detected 14 different noise factors, classified into one of two major categories: *local* or *global*, as they affect exclusively image regions or the complete image. The *local* category is comprised of iris obstructions, reflections, off-angle, and partial images, while the *global* comprises poor focused, motion-blurred, rotated, improper lighting, and out-of-iris images. Examples of the UBIRIS.v2 noise factors are given in Fig. 3. It presents a close-up iris image with good quality (Fig. 3a) and images that contain at least one of the aforementioned noise factors (Figs. 3b, 3c, 3d, 3e, 3f, 3g, 3h, 3i, 3j, 3k, 3l, 3m, 3n, and 3o).
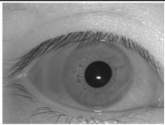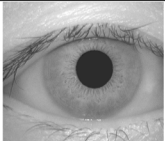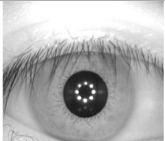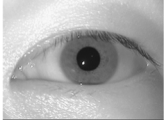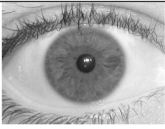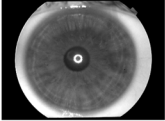
3.3 Statistical Significance of the UBIRIS.v2 Database

In this section, we address the problem of whether the experiments performed on the UBIRIS.v2 database produce statistically significant results.

Let α be the confidence interval. Let P be the error rate of a classifier and $\hat{P}$ be the estimated error rate over a finite number of test patterns. At an α-confidence level, we want the true error rate not to exceed the estimated error rate by an amount larger than $\varepsilon(N, \alpha)$. Guyon et al. [11] fixed $\varepsilon(N, \alpha) = \beta P$ to be a given fraction of P. Assuming that recognition errors are Bernoulli trials, authors concluded that the number of required trials N to achieve $(1 - \alpha)$ confidence in the error rate estimate is $N = -ln(\alpha)/(\beta^2 P)$. A typical value for α is 0.05 and a typical

---

TABLE 1
Comparison between the Iris Image Databases That Are Freely Available for Biometric Purposes

Database	Example Image	Total Images	Wavelength	Varying Distances	Acquisition Device	Observations
BATH		16 000	Near Infrared	No	ISG LightWise LW-1.3-S-1394	High homogeneous lighting environment. Contains essentially iris obstructions due to eyelids and eyelashes.
CASIA.v1		756	Near Infrared	No	CASIA camera	Previous filling of the pupil regions turns segmentation much more easier. High reputable journals now automatically reject papers which experiments were exclusively performed on this version of the database.
CASIA.v2		2 255	Near Infrared	No	CASIA camera	Subset of the subsequent database version.
CASIA.v3		22 051	Near Infrared	No	OKI irispass-h	Images captured with two different devices. Contains images with close characteristics to the v1 version, with exception of the manual pupil filling.
ICE 2005		2 900	Near Infrared	No	LG EOU 2200	Contains off-angle iris images. Intensity values automatically stretched to 171 levels.
ICE 2006		75 000	Near Infrared	No	LG EOU 2200	Contains off-angle, partial, rotated and non-iris images and eyes with contact lenses. Intensity values automatically stretched to 171 levels.
MMU.1		450	Near Infrared	No	LG EOU 2200	Noise factors avoided.
MMU.2		995	Near Infrared	No	Panasonic BM-ET100US	Noise factors avoided.
UBIRIS.v1		1 877	Visible	No	Nikon E5700	Images captured under heterogenous lighting environments. Several reflections and obstructions can be observed.
UPOL		384	Visible	No	SONY DXC-950P 3CCD with TOPCON TRC50IA	Completely noise-free images acquired with an optometric framework under high constrained environment.
WVU		3 099	Near Infrared	No	OKI irispass-h	Contains poor lighting, defocus blur, off-angle, and heavy occluded images.

value for β is 0.2. Based on these values, Guyon et al. [11] recommended the simpler form $N \approx \frac{100}{P}$.

We had a varying number of subjects that offered to be volunteers for the first, second, and for both imaging sessions. However, assuming that each iris image can be used to generate a biometric template, the remaining images from the same eye can be used to analyze intraclass variability, and the remaining images from different eyes can be used to analyze interclass variability, it is possible to obtain a bound for the error that it is possible to test with statistical significance.

TABLE 2
Details of the UBIRIS.v2 Images of the Image Acquisition Framework
and Setup and of the Subjects That Offered Themselves
as Volunteers to the Imaging Sessions

Image Acquisition Framework and Set-Up	
Camera = Canon EOS 5D	Color Representation = sRGB
Shutter Speed = 1/197 sec.	Lens Aperture = F/6.4 - F/7
Focal Length = 400 mm	F-Number = F/6.3 - F/7.1
Exposure Time = 1/200 sec.	ISO Speed = ISO-1600
Metering Mode = Pattern	
Details of the Manually Cropped Resultant Images	
Width = 800 pixels	Height = 600 pixels
Format = tiff	Horizontal Resolution = 72 dpi
Vertical Resolution = 72 dpi	Bit Depth = 24 bit
Volunteers	
Totals = Subjects 261; Irises 522; Images 11 102	Gender = Male: 54.4%; Female: 45.6%
Age = [0,20]: 6.6% [21,25]: 32.9% [26,30]: 23.8% [31,35]: 21.0% [36,99]: 15.7%	Iris Pigmentation Light : 18.3% Medium : 42.6% Heavy : 39.1%

The 11,102 images of the UBIRIS.v2 database enable, respectively, 127,746 and 61,482,804 intra and interclass comparisons. This guarantees statistical significance in experiments with an empirical error rate $\hat{P}$ down to $1{,}623 \times 10^{-6}$ percent. However, we stress that this is a lower bound value that would be increased if we do not assume the independence between images and error correlations are taken into account.

4   EXPERIMENTS

To enhance the singular characteristics of the UBIRIS.v2 database, some experiments were carried out. This section describes how we estimated the image quality and analyzes the separability between intra and interclass comparisons, regarding the imaging distance and the level of iris pigmentation.

4.1   Image Quality Assessment

In the scope of the NICE.I [26] contest, we manually discriminated between the noise-free iris regions and the remaining data on a training set delivered to participants. This was carried out on 1,000 randomly selected iris images. As illustrated in Fig. 4, for each
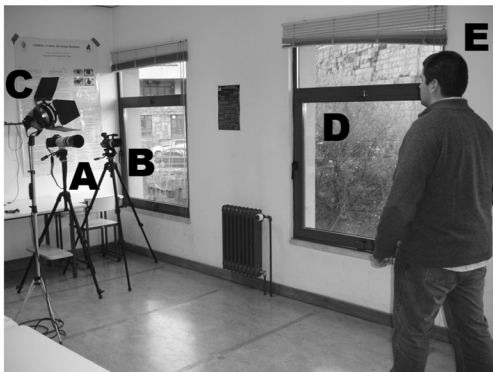

Fig. 1. Overview of the used image acquisition framework (A, B), light sources (C, D), and subjects location (E).
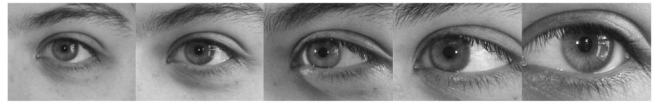

Fig. 2. Examples of close-up iris images acquired at-a-distance, on-the-move (between 8 and 4 meters), and under high dynamic lighting conditions.

of these, we built the corresponding binary map that distinguishes between the above referred two types of data. We considered that a portion of the iris is "noisy" if it is occluded by any type of local noise factor and the underlying appearance of the iris texture cannot be evidently seen by human inspection. These maps were the basis of our experiments and assure that failures in the eye detection, iris segmentation, and noise discrimination stages do not occur.

4.1.1   Image Dimensions

The error rates of any iris-based biometric system will mainly depend on the amount of information existent in the captured data and on the proportion of noise that obstructs the underlying texture and corrupts the discriminating information.

In order to establish a relationship between the image acquisition distance and the maximum amount of iris data that it is possible to capture with the used image acquisition framework and setup, we measured the average iris diameter of frontal images as the image acquisition distance varies. The obtained results are given in Fig. 5a and indicate that the diameter of the captured irises varies according to an inverse logarithmic function. Through trial-and-error interpolation, we obtained the following coarse approximation function $d(x) : \mathbb{R}^+ \to \mathbb{R}^+$:

$$d(x) \approx \frac{150}{ln(\frac{x}{1.85})}, \qquad (1)$$

where x is the image acquisition distance (in meters) and $d(x)$ is the average diameter of the captured irises. This is confirmed in Fig. 5b, which gives the image resolution in the iris regions, where the shaded areas represent the 95 percent confidence intervals. Results were obtained through the division of the number of pixels that fall into the iris region by an iris area of 0.785 cm^2, averaged from human eye morphology studies that are publicly available. These observations confirm that the aforementioned acquisition framework and setup enable the capturing of sufficient data to perform iris recognition, as nearly 50 percent of the database images have iris diameters close to the lower bound (140 pixels) recently proposed by Daugman [6].

Regarding the proportion of occluded data within the iris ring (Fig. 4), we divided the number of noise-free iris pixels by the total that ideally should fall within the iris ring, obtaining the values shown in the histogram of Fig. 6a. The horizontal axis denotes the proportion of noise-free pixels and the vertical axis the respective probability of occurrence in the database. We observed that—on average—25-30 percent of the pixels that fall within the iris ring were corrupted by one of the local noise factors. Also, just about 3 percent of the images are completely noise-free, while around 0.9 percent contain full noisy data, correspondent to out-of-iris images or imaged in extremely poor lighting conditions.

4.1.2   Image Information

To characterize image textures, we used the *image entropy*, a statistical randomness measure widely used in the image processing domain. According to the conclusion reported by He et al. [12], we considered the levels of iris pigmentation as a factor that influences the amount of discriminating information captured for biometric purposes.

Let I be a gray-scale image with g gray levels and $p(k)$ be the probability of occurrence of the gray level k in I. The image
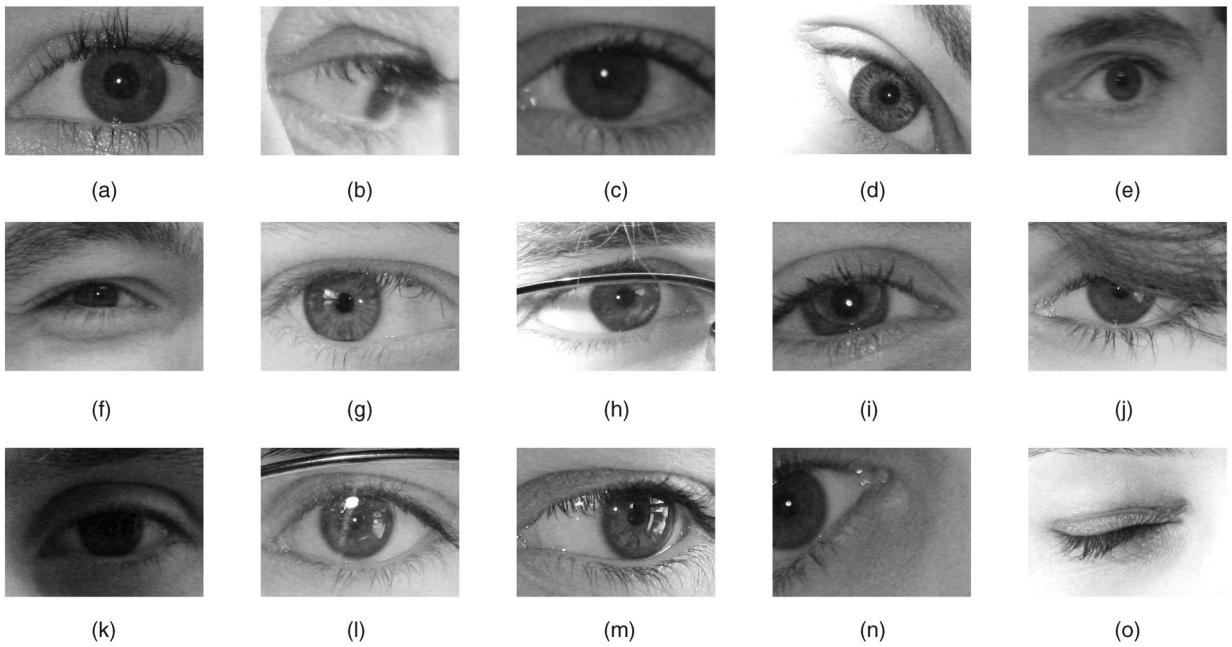
Fig. 3. Comparison between a good quality image and several types of nonideal images of the UBIRIS.v2 database. These images are the result of less constrained imaging conditions, either under varying lighting conditions, at-a-distance, and on-the-move. (a) Good quality iris image. (b) Off-angle iris image. (c) Poorly focused iris image. (d) Rotated iris image. (e) Motion-blurred iris image. (f) Iris obstructions due to eyelids. (g) Iris obstructions due to eyelashes. (h) Iris obstructions due to glasses. (i) Iris obstructions due to contact lenses. (j) Iris obstructions due to hair. (k) Iris imaging in poor lighting conditions. (l) Iris with specular reflections. (m) Iris with lighting reflections. (n) Partially captured iris. (o) Out-of-iris image.

entropy h is given by $h(I) = -\sum_0^{g-1} p(k)log_2(p(k))$. Let B be the binary noise map correspondent to I, as illustrated in Fig. 4. Thus, $B(x,y) = 0$ or 255 whether the respective pixel (x,y), respectively, belongs to the iris ring and is noise-free or not. The *entropy of the iris region* $ih(.)$ of I is obtained taking exclusively into account pixels (x_i, y_i) such that $B(x_i, y_i) = 0$, i.e., the noise-free iris data. Finally, for normalization purposes, we divided the entropy value by the area of the noise-free iris region:

$$ih(I) = \frac{h(I(x,y)|B(x,y)=0)}{\mathbb{I}_{\{B(x,y)=0\}}}, \qquad (2)$$

where $\mathbb{I}_{\{.\}}$ is the characteristic function.

The obtained values are given in Fig. 6b. The horizontal axis corresponds to the imaging distance and the vertical axis to the entropy value. Data points give the observation average values for *light* (continuous series), *medium* (dotted series), and *heavy* pigmented irises (dashed series), as a function of the imaging distance. The shaded areas represent the 95 percent confidence intervals. It can be confirmed that the average entropy of the iris data decreases inversely with the imaging distance, and more evidently, with the levels of iris pigmentation.

4.2 At-a-Distance and On-The-Move Recognition

The small probability of false matches in the comparison between iris signatures has been widely reported, and this fact is regarded as one of the major advantages of the iris when compared to other biometric traits. However, a fundamental hypothesis for the feasibility of at-a-distance and on-the-move iris recognition remains to be verified: to assure that the comparison between templates extracted from good quality data and samples extracted from partial or noniris regions (due to hypothetic failures on the eye detection and segmentation modules) will not frequently produce false matches. To test this hypothesis, we used the recognition method proposed by Daugman [6] and performed a comparison between 1,000 templates extracted from good quality iris images and 10,000 sample signatures, extracted from randomly cropped noniris or partial iris regions. Additionally, we used a set of 10,000 natural and synthetic texture images, performing a total of 20,000,000 comparisons ($1,000 \text{ templates} \times 20,000 \text{ samples}$). Fig. 7a exemplifies some of the images from where we extracted the biometric signature samples.

Fig. 7b gives the histogram of the obtained dissimilarity scores s (vertical bars) and the approximated normal distribution (line plot
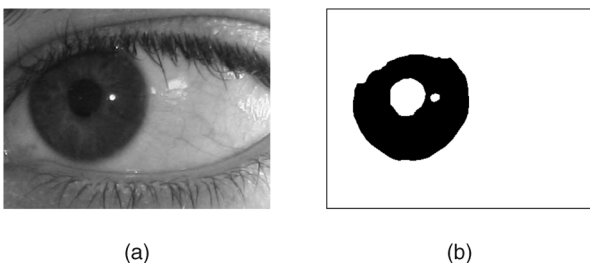
Fig. 4. Example of a manually built binary map that distinguishes between the noise-free iris regions and all the remaining types of data. (a) Noisy iris image. (b) Corresponding binary noise map.
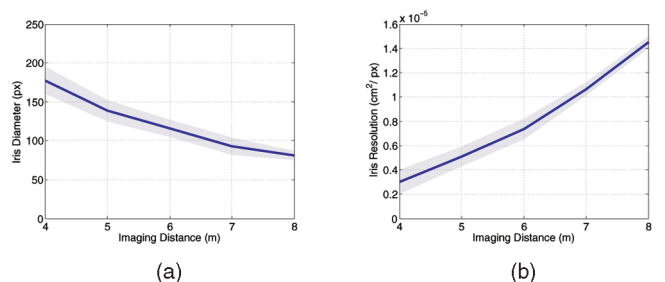
Fig. 5. Maximum amount of information possible to acquire at-a-distance and on-the-move through the image acquisition framework and setup used. (a) Average diameters of the captured irises as a function of the image acquisition distance. (b) Average image resolution at the iris regions as a function of the image acquisition distance.
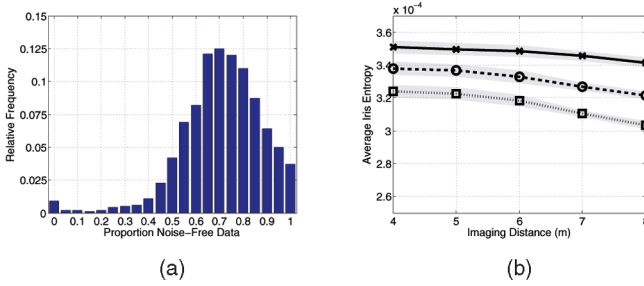
(a)   (b)

Fig. 6. (a) Proportion ($[0, 1]$) of noise that occludes the iris texture and (b) average entropy of the noise-free iris regions as a function of the levels of iris pigmentation. Light, medium, and heavy pigmented irises are represented by the continuous, dotted, and dashed lines.
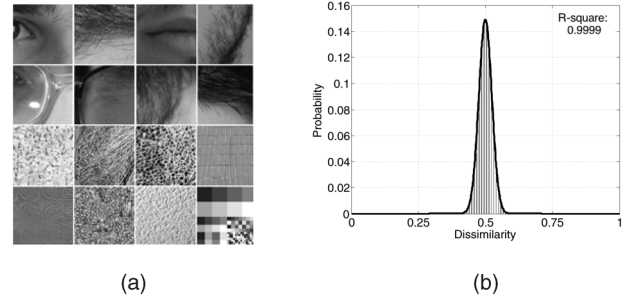

(a)   (b)

Fig. 7. Histogram of the dissimilarity scores between iris templates acquired from relatively good quality data and partial or noniris data. (a) Simulation of failures in the eye detection and iris segmentation stages. (b) Dissimilarities between signatures extracted from iris and noniris or partial iris images.

with $\mu = 0.49992$ and $\sigma = 0.02419$). We confirmed that the iris encoding and comparison strategies used produce a false match almost with null probability ($P(s < 0.33) \approx 1.03 \times 10^{-12}$). Thus, it can be assured with extremely high confidence that such recognition systems will not produce false matches and that any reported match is very likely genuine. Obviously, the existence of false nonmatches will be unavoidable due to extreme lighting variations, movements, and perspectives.

In order to perceive the separability between intra and interclass comparisons and infer the potential sensitivity that such recognition systems could achieve, we divided the 1,000 iris images previously used to extract the templates into three subsets: light, medium, and dark irises. All of these images are frontal and practically noise-free, acquired under good lighting conditions. The signatures extracted from these images were then compared with 1,000 sample signatures extracted from images with corresponding iris pigmentation levels. Results are given in Fig. 8, where the horizontal axis represents the dissimilarity values and the vertical the respective probability. The light and dark bar series give, respectively, the intra and interclass comparisons. The separability between intra and interclass comparisons is evident, which constitutes a good indicator toward the feasibility of the type of biometric recognition discussed in this paper. However, we confirmed the relevant role played by the levels of iris pigmentation with the values obtained for a Fisher-ratio test τ [8]

$$\tau = \frac{\mu_E - \mu_I}{\sqrt{\frac{1}{2} \left(\sigma_E^2 + \sigma_I^2 \right)}}, \tag{3}$$

where μ_I, μ_E and σ_I, σ_E are, respectively, the means and standard deviations of the inter and intraclass comparisons.

Finally, we obtained a bound for the maximal sensitivity that the discussed recognition process could achieve with full specificity. This value was estimated through the proportion of intraclass

comparisons below the minimal interclass dissimilarity value, having obtained, respectively, 0.911, 0.773, and 0.586 values for the light, medium, and dark irises. Although these values are far from those obtained in the constrained NIR mode, the key point is that the described image acquisition process could be performed covertly. Thus, any reported match should be considered positive since it came from a situation where no human effort was required.

5   DATABASE AVAILABILITY

The value given to the UBIRIS.v2 database should have direct correspondence with the number of persons that use it in their experiments. Thus, we decided to make UBIRIS.v2 public and freely available through the UBIRIS databases Web site (http://iris.di.ubi.pt). On 1 June 2009, the complete database will be freely available for academic and research purposes at the above referred Web site. Moreover, the binary maps that distinguish between the noise-free iris regions and all the remaining data of 1,000 randomly selected images will also be available for download.

6   CONCLUSIONS

In this paper, we announced the availability of the UBIRIS.v2 iris image database and described the used imaging framework and acquisition protocol. We highlighted the most discriminating points between this database and others with similar purposes, specifically the fact that it contains images captured on the visible wavelength at-a-distance and on-the-move. Also, we gave results about the amount of information that it is possible to capture through the used acquisition setup, reported measures of separability between the resultant iris signatures, and confirmed the major impact that the levels of iris pigmentation have in the recognition feasibility. We think that the UBIRIS.v2 database is a
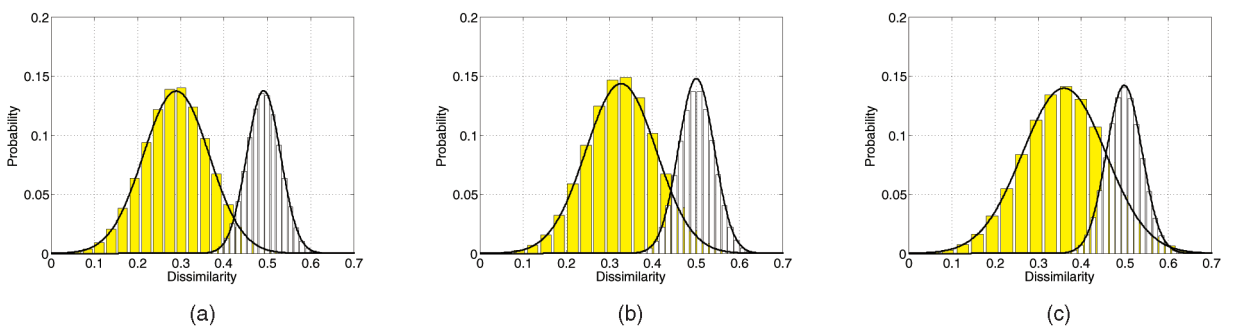

(a)   (b)   (c)

Fig. 8. Separability between intra and interclass comparisons regarding the levels of iris pigmentation. (a) "Light" pigmented Iiris, $\mu_I = 0.290$, $\sigma_I = 0.076$, $\mu_E = 0.492$, $\sigma_E = 0.039$, $\tau = 2.350$. (b) "Medium" Pigmented Iris, $\mu_I = 0.327$, $\sigma_I = 0.081$, $\mu_E = 0.501$, $\sigma_E = 0.041$, $\tau = 1.994$. (c) "Heavy" Pigmented Iris, $\mu_I = 0.360$, $\sigma_I = 0.0968$, $\mu_E = 0.499$, $\sigma_E = 0.0417$, $\tau = 1.317$

valuable tool for the specification of the limits for the visible wavelength and nonconstrained iris recognition, namely, the required lighting conditions, imaging distance, subject movements, and perspectives. Finally, we concluded that the discussed type of recognition is also conditioned by the development of alternate iris segmentation and noise detection strategies, able to deal with a higher range of data heterogeneity.

ACKNOWLEDGMENTS

REFERENCES

[1] Atos Origin, UK Passport Service, Biometrics Enrollment Trial, http:\\www.ukpa.gov.uk\publications.asp, 2005.
[2] W.W. Boles and B. Boashash, "A Human Identification Technique Using Images of the Iris and Wavelet Transform," *IEEE Trans. Signal Processing,* vol. 46, no. 4, pp. 1185-1188, Apr. 1998.
[3] K. Bowyer, K. Hollingsworth, and P. Flynn, "Image Understanding for Iris Biometrics: A Survey," *Computer Vision and Image Understanding,* vol. 110, no. 2, pp. 281-307, 2008.
[4] C. Boyce, A. Ross, M. Monaco, L. Hornak, and X. Li, "Multispectral Iris Analysis: A Preliminary Study," *Proc. IEEE CS Workshop Biometrics at the IEEE Conf. Computer Vision and Pattern Recognition,* pp. 51-59, June 2006.
[5] Y. Chen, S. Dass, and A. Jain, "Localized Iris Quality Using 2D Wavelets," *Proc. Int'l Conf. Biometrics,* pp. 373-381, Aug. 2006.
[6] J.G. Daugman, "How Iris Recognition Works," *IEEE Trans. Circuits and Systems for Video Technology,* vol. 14, no. 1, pp. 21-30, Jan. 2004.
[7] J.G. Daugman, "New Methods in Iris Recognition," *IEEE Trans. Systems, Man, and Cybernetics—Part B: Cybernetics,* vol. 37, no. 5, pp. 1167-1175, Oct. 2007.
[8] R.O. Duda and P.E. Hart, *Pattern Classification and Scene Analysis.* Wiley, 1973.
[9] M. Dobes and L. Machala, UPOL Iris Image Database, http://phoenix.inf.upol.cz/iris/, 2004.
[10] C. Fancourt, L. Bogoni, K. Hanna, Y. Guo, R. Wildes, N. Takahashi, and U. Jain, "Iris Recognition at a Distance," *Proc. 2005 IAPR Conf. Audio and Video Based Biometric Person Authentication,* pp. 1-13, July 2005.
[11] I. Guyon, J. Makhoula, R. Schwartz, and V. Vapnik, "What Size Test Set Gives Good Error Rate Estimates?" *IEEE Trans. Pattern Analysis and Machine Intelligence,* vol. 20, no. 1, pp. 52-64, Feb. 1998.
[12] Y. He, J. Cui, T. Tan, and Y. Wang, "Key Techniques and Methods for Imaging Iris in Focus," *Proc. IEEE Int'l Conf. Pattern Recognition,* pp. 557-561, Aug. 2006.
[13] Y. Huang, S. Luo, and E. Chen, "An Efficient Iris Recognition System," *Proc. First Int'l Conf. Machine Learning and Cybernetics,* pp. 450-454, Nov. 2002.
[14] Institute of Automation, Chinese Academy of Sciences, CASIA Iris Image Database, http://www.sinobiometrics.com, 2004.
[15] International Biometric Group, Independent Test of Iris Recognition Technology, http://www.biometricgroup.com/reports, 2005.
[16] N.D. Kalka, J. Zuo, V. Dorairaj, N.A. Schmid, and B. Cukic, "Image Quality Assessment for Iris Biometric," *Proc. 2006 SPIE Conf. Biometric Technology for Human Identification,* pp. 61020D-1-62020D-11, Apr. 2006.
[17] L. Ma, T. Tan, D. Zhang, and Y. Wang, "Local Intensity Variation Analysis for Iris Recognition," *Pattern Recognition,* vol. 37, no. 6, pp. 1287-1298, 2004.
[18] T. Mansfield, G. Kelly, D. Chandler, and J. Kane, *Biometric Product Testing Final Report,* Issue 1.0, 2001.
[19] J.R. Matey, D. Ackerman, J. Bergen, and M. Tinker, "Iris Recognition in Less Constrained Environments," *Advances in Biometrics: Sensors, Algorithms and Systems,* pp. 107-131, Springer, Oct. 2007.
[20] Multimedia University, MMU Iris Image Database, http://pesona.mmu.edu.my/ccteo, 2004.
[21] R. Narayanswamy, G. Johnson, P. Silveira, and H. Wach, "Extending the Imaging Volume for Biometric Iris Recognition," *Applied Optics,* vol. 44, no. 5, pp. 701-712, Feb. 2005.
[22] National Institute of Standards and Technology, Iris Challenge Evaluation, http://iris.nist.gov/ICE/, 2006.
[23] National Institute of Standards and Technology, MBGC Multi Biometric Grand Challenge, http://face.nist.gov/mbgc/, 2007.
[24] K. Park and J. Kim, "A Real-Time Focusing Algorithm for Iris Recognition Camera," *IEEE Trans. Systems, Man, and Cybernetics,* vol. 35, no. 3, pp. 441-444, Aug. 2005.
[25] H. Proença and L.A. Alexandre, "UBIRIS: A Noisy Iris Image Database," *Proc. 13th Int'l Conf. Image Analysis and Processing,* pp. 970-977, Sept. 2005.
[26] H. Proença and L.A. Alexandre, "The NICE.I: Noisy Iris Challenge Evaluation, Part I," *Proc. IEEE First Int'l Conf. Biometrics: Theory, Applications, and Systems,* pp. 27-29, Sept. 2007.
[27] A. Ross, S. Crihalmeanu, L. Hornak, and S. Schuckers, "A Centralized Web-Enabled Multimodal Biometric Database," *Proc. 2004 Biometric Consortium Conf.,* Sept. 2004.
[28] S. Schuckers, N. Schmid, A. Abhyankar, V. Dorairaj, C. Boyce, and L. Hornak, "On Techniques for Angle Compensation in Nonideal Iris Recognition," *IEEE Trans. Systems, Man, and Cybernetics, Part B,* vol. 37, no. 5, pp. 1176-1190, Oct. 2007.
[29] Univ. of Bath, University of Bath Iris Image Database, http://www.bath.ac.uk/elec-eng/pp./sipg/, 2004.
[30] R.P. Wildes, "Iris Recognition: An Emerging Biometric Technology," *Proc. IEEE,* vol. 85, no. 9, pp. 1348-1363, Sept. 1997.

▷ **For more information on this or any other computing topic, please visit our Digital Library at** www.computer.org/publications/dlib.